Spectrum Journal of Innovation, Reforms and Development
Volume 35, January- 2025 | ISSN (E): 2751-1731
WEBSITE: WWW.SJIRD.JOURNALSPARK.ORG

IDENTIFYING THE THERMAL PARAMETERS OF DIESEL ENGINE USING DIESEL FUEL AND SOYBEAN METHYL ESTER BLENDS

Wisam Al-Obaidi*1,
Ahmed M. Hassan 1
Husam Kareem Mohsin Al-Jothery1
Dhafer A. Hamzah1
1Mechanical Engineering Department,
University of Al-Qadisiyah, Al-Diwaniyah 58001, Qadisiyah, Iraq
*Corresponding Author Email: wisam.jasim@qu.edu.iq

Abstract
This work examines numerically the use of soybean methyl ester (SME) biodiesel along with diesel in a constant-speed, single-cylinder diesel engine. Two fuels were tested: 20%SME and pure SME, besides a baseline neat diesel for comparison. The simulation software Diesel-RK was used in this study, which is based on the multizone combustion model. The results obtained for selected biodiesel showed a quicker start of combustion due to the reduction in the delay period, which is impacted by cetane number. Compared to diesel, the SMD was increased by 8.7% and 24% for the use of 20% SME and SME, respectively. The brake thermal efficiency (BTE) was decreased by 0.8% for 20%SME while it decreased by 6.62% with the use of pure SME. Remarkable reduction in the nitrogen oxides (NOx) emissions was reported with the use of SME by 50% compared to diesel fuel. The carbon dioxide (CO2) emissions were increased as a result of using SME blends with diesel. The comparison between obtained findings with the result of other studies reported an accepted deviation.

Keywords: SME Biodiesel; Combustion; Diesel-Rk software; NOx; Pollutant emissions.

Introduction

The enormous increase in the population worldwide, air pollution due to using fossil fuel/exhaust emissions, global warming, and demands for efficient diesel engines represent key factors that escalate the issue of climate change. Such a big dilemma faces all countries has prompted the researchers to find alternative source of sustainable fuel such as biodiesel fuel. Biodiesel is usually produced by transforming vegetable oils (soybean/rapeseed oils) or animal fats into fatty acid methyl esters[1] [2].

Various experimental and numerical studies were conducted to study the characteristics of diesel engines[3], nozzle dimeter, ignition delay, injection timing etc. using different biofuels [4]. Gupta et al. [5] investigated the feasibility of using kapok oil, microalgae and soybean oil as alternative of feedstock in diesel engines. The obtained results of blending 20% kapok oil, microalgae and soybean with diesel were employed to evaluate the emission and output of the engine. The brake thermal efficiency was inclined by (2%) 20% microalgae/80% diesel, (1.5%) 20% kapok /80% diesel and (2%) 20% soybean oil/80% diesel compared to pure diesel. On the other hand, Specific

fuel consumption was revealed to growth by 3.8% for (20% kapok/ 80% diesel) blend. Using blends of (20% microalgae/ 80% diesel) and (20% soybean /80% diesel) showed a good reduction in the emissions of NOx and soot by (10.0% and 14.2%) and (10.0% and 4%) respectively.

The production of biodiesel can be obtained from various animal or vegetable raw materials that ensure a good oxidative stability to reduce the emissions of CO_2 [6] [7]. Comparison of diesel and biodiesel fuels showed that their thermal energy is the similar. Thus, converting waste (animal or vegetable) oils into biodiesel fuel presents a good source of sustainable fuel [8]. Moreover, biodiesel is rich in the content of oxygen and has deficiency in minerals and sulfur, therefore, produces low exhaust emissions. The biodiesel can be obtained from three sources depending on the raw materials [9]: (soybean, sunflower, rapeseed, and oil plants) , (vegetables oils and animal fats) and (wood chips, straw, microbial grease and solid waste). The most usable of biodiesel in research work among the other fuels is soy methyl ester in pure liquid form [10]. Vázquez-Garrido [11] and his group studied five operative conditions in a fixed_bed continuous flow micro reactor of waste/new soybean oil to produce biofuel employing ($NiMo/Al_2O_3$) catalyst. The key variances between the new and the waste oil are fatty acid concentration and the peroxide values. The finding showed formation of waxes and conversion of triglycerides highly depend on mass catalyst (0.1 g), the concentration of soybean oil (0.104 mol/L) and temperature (T = 380 °C). In addition, both waste and new soybean oil produced biofuel comprises of four hydrocarbons of (n-C15), (n-C16), (n-C17) and (n-C18), in which (n-C17) has the greatest concentration in both oils.

He et al.[12] produced biodiesel by effective transesterification process of waste soybean oil using Mo catalyst maintained on exterior surface of (Silicalite_1 [Mo/S_1_p] zeolite). The findings showed that (5Mo/S_1_p) catalyst performed well and stable, which unveiled the waste soybean oil conversion of (80.73%) and biodiesel electivity of (99.32%). Thus, the obtained synthesized-biodiesel showed good properties as low priced sustainable fuel compared to international standards. De Poures et al. [13] conducted experiments using response surface method to improve the exhaust gas recirculation, performance, minimize emissions and fuel injection timing in a direct injection diesel engine using blend of triple fuels (30 biodiesel/ 20 (1-hexanol)/ 50 diesel). By considering the pure diesel is the reference and at optimal conditions, it was found an increase in the carbon monoxide, hydrocarbon, and smoke, however, a remarkable decrease in the NOx emissions. In addition, involving methyl ester in the blends showed decrease in CO, NOx, HC and smoke emissions. Elkelawy et al. [14] employed transesterification process using catalyst to convert blends of soybean and sunflower oils into methyl esters. The results showed that (5%) of error rate in brake-specific energy consumption and thermal efficiency throughout a validation process for all blends of biodiesel. Mora et al. [15] used LiOH catalyst in the production process of soybean oil biodiesel. The following parameters operation-time, methanol/oil ratio, and catalyst-loading were investigated. The results showed the significance of parameters as follows: methanol/oil ratio > operation-time > catalyst-loading and reasonably predicted the optimal condition (operation-time = (1.2 h), methanol/oil ratio = (8.9:1), and catalyst-loading = (1.08% wt.)) resulting in (98.8%) fatty acid methyl ester yield. Thus, the produced fatty acid methyl ester is comparable with standards of European biodiesel

Santos Sonnemberg et al. [16] performed a study to evaluate the action of antioxidant between biodiesel blend of (70% soybean oil/ 30% animal fat) and metal. The findings of the curcumin antioxidant revealed a good efficiency by absorption at (425 nm), IP values larger than (8 h). it

can be concluded that curcumin behaves a good antioxidant even in the circumstances of exposing biodiesel to intensive oxidative. Aleman-Ramirez et al. [17] reported the process of using ash obtained from agro-industrial waste at 500 c for (2 hours) as a reusable catalyst, due to high basicity , existence of potassium chloride, to harvest biodiesel from vegetable oils (sunflower and soybean). During the optimum reaction conditions: 240 min reaction time, (3 wt%) and (5 wt%) of catalyst charge and ratio of (methanol/oil molar) of (6:1 soybean) and (9:1 sunflower), the catalyst successfully achieved about 92% conversion of the both oils into biodiesel fuel. Ağbulut et al. [18] proposed a transesterification process combined with various hybrid catalysts to convert the waste of used soybean oil into biodiesel fuel. The parameters used in the transesterification process were as follow: reaction time from (15 to 75 h) and velocities of flow from (0.3 to 1.5 mL/min). the observed results showed that blend of (25% diesel and 75% soybean oil) produced (17.96%) smoke less than diesel, and produced (30.05 %) BTE which is closer the BTE of diesel (30.81%).

The practical using of hydrogenated-catalytic biodiesel and fatty-acid methyl-ester in light duty engines were demonstrated in many comparative studies. For instance, Zhong et al. [19] experimentally studied and compared the emissions and combustion performance of (hydrogenated catalytic biodiesel, fatty acid methyl ester ,diesel) blends for a steady state cycle. The obtained findings showed that the blends of pure diesel and 80% diesel, 20% hydrogenated gained high value of peak cylinder pressure, low ignition delay time and CA50. However, blends of 80% diesel, 20% biodiesel gained low values of peak cylinder pressure and CA10. In terms of brake specific fuel consumption, all blends showed low values, for example, BSFC of (80% diesel, 20% biodiesel) was higher than BSFC of pure diesel of (1.49%) in contrast to the BSFC of (80% diesel, 20% hydrogenated). The emissions of CO_2 and NOx reported to be the lowest among all the blends in mode 8.

Gavhane et.al [20] experimentally studied the impact of silica on the emissions and performance of an engine fueled with soybean methyl-ester. Various loading conditions and samples of fuel blends were employed (100% pure diesel, 25% soybean methyl-ester, 25% soybean methyl-ester/ 25% silica, 25% soybean methyl-ester/ 50% silica, and 25% soybean methyl-ester/ 75% silica). Addition of silica to soybean methyl-ester showed an apparent increase in the BSFC and BTE values around (3.48–6.39%) (5.81–9.88%) respectively compared to 25% soybean methyl-ester. However, blends of silica with soybean methyl-ester decreased the smoke (10.16–23.54%), HC (20.56–27.5%), and CO (1.9– 17.5%) emissions. Kumar dep et al. [21] conducted an experiment to evaluate the emission and efficiency of diesel engine utilizing different blends of diesel and palm-kernel oil methyl-ester. Blends of 20% biodiesel and full load was reported to be the best due to the highest decrease in the NOx, HC and BSFC values, and increase in the brake thermal efficiency at ultimate performance index of 0.809. Zhang et al. [22] developed a numerical study using reduction mechanism of compact biodiesel oxidation of low temperature biodiesel combustion relying on five biodiesel methyl esters. The first part of the study illustrated the auto-ignition of biodiesel/air blend for different initial conditions. There was a comparison made between the predicted and experimental results that showed inconsistencies in the ignition-delay in the orders of milliseconds. Good agreement was shown in terms of mixture temperature and mole fraction, implying that the reduction mechanism keeps the crucial reaction trails of the original-mechanism. Hasnain et al. [23] prepared a biofuel by mixing (100% soy-methyl ester),

(50% soy-methyl ester/ 50% methyl oleate) and diesel to be investigated using common rail-direct-injection engine. The obtained results showed that low value in BSFC when enriched biodiesel is utilized compared to 100% soy-methyl ester. The average values of BSFC were 30% (100% soy-methyl ester) and 14.9% (50% soy-methyl ester/ 50% methyl oleate) higher than BSFC of pure diesel. 100% soy-methyl ester gained the lowest BTE value among the blends. Emissions of NOx were shown to be higher in biodiesel blends than emissions of in diesel resulting short ignition delay.

Ramalingam et al. [24] experimentally studied the Capparis Spinosa Methyl Ester in a single cylinder duel fuel (hydrogen-diesel) engine with multi_walled multi_additive nanotubes. The results showed that employing hydrogen of flowrates (5 and 10 lpm) improves the performance and combustion characteristics. Furthermore, blending hydrogen and Capparis Spinosa Methyl Ester enhance remarkably the BTE (2.52% - 4.52%), BSFC (1.8% - 2.2%) and decrease the ignition delay and emissions of HC (7.2% -13.1%), CO (8.3% - 13.4%) except emission of NOx (4.82% -8.16%). Combination of Capparis Spinosa Methyl Ester and multi_walled multi_additive nanotubes showed lower ignition delay, HC emissions, (BSFC) and higher (BTE). Al-Dawody et al. [25] numerically evaluated the influence of engine thermal parameters for blending beef Tallow methyl ester (10%, 20% and 30%) with diesel using multizone combustion model. The results revealed minor decrease in the heat release, pressure and shorter ignition delay for all fractions compered to pure diesel. However, an increase of (68%, 3.34% and 5%) was shown in the Sauter-mean diameter of the droplets in all three blends of beef Tallow methyl ester and similarly for BSFC (1.68%, 3.34% and 5%).

The broad demand for using biodiesel as alternative to the ordinary fuel, the effect of biodiesel combustions must be studied and evaluated thoroughly. Yusuff et al. [26] used ethanol, methanol and mixed methanol/ethanol to produce biodiesel from cooking oil. compression ignition engine of three samples of 20% (biodiesel ethanol, biodiesel methanol, biodiesel ethanol/ methanol) were examined and evaluated. The results showed that alkyl (methyl/ethyl) ester component in all three samples were 97.72% for biodiesel methanol, 91.83% for biodiesel ethanol and 84.65% for biodiesel ethanol/ methanol. Emissions of CO for 20% biodiesel methanol blend were shown to be lower compared to pure biodiesel, 20% biodiesel ethanol and 20% biodiesel ethanol/ methanol. However, the pure biodiesel observed to show the lowest NOx emissions.

Al-iessa et al. [27] carried out a study using molecular dynamics approach to demonstrate the influence of oxide nanoparticles of (aluminum/copper) on the thermal performance of biodiesel (Soy methyl ester) as a base fluid. A noticeable improvement in the thermal efficiency and conductivity were seen for the base fluid by the addition of nanoparticles. Passos et al. [28] evaluated enzymatic degumming of the crude soybean oil who previously optimized [29]. The approach of enzymatic degumming during the production of biodiesel was found necessary to avoid the impurities and obtaining high quality biodiesel fuel. Kumar and Bansal [30] employed the response surface methodology to build a regression model the parameters of soybean biodiesel having reaction duration (30–60 min), catalyst concentration (NaOH of 1–2% w/w) and the molar ratio (of 6–12). A significant value of (R2) was found of (0.9411), while the (R2) value of the training was (0.9918) which means the model accurately link the input parameters with the biodiesel yield. Chen et al. [31] numerically studied the combustion performance and the impact of using nano particles (Al_2O_3 and CuO) with various volume fractions on methyl ester biodiesel.

The findings showed that addition of CuO obtained good thermal performance compared to Al_2O_3. Moreover, the heat flux of the nano fluids (Al_2O_3 and CuO) was (2410.31) W/m^2 and (2410.31) W/m^2, respectively. Tosun et al.[32] investigated the effects of blending hydrogen with soybean biodiesel with alumina nanoparticles on the emissions and performance of diesel engines. The addition of nanoparticles to the blend of hydrogen can improve the performance of the engine and emits low emissions compared to the biodiesel/diesel fuel only. However, NOx emissions were seen to be higher in all blend compared to diesel fuel. Blending 20% of biodiesel, hydrogen and 80% diesel, an improvement was seen of (6.64%) in power and BSFC value was decreased by (2.72%) compared to pure diesel.

Gurusamy and Subramanian [33] investigated the addition of hydrogen (5 to 20 LPM) to the cottonseed oil methyl ester as a fuel in diesel engine at different load conditions and a constant speed. The results showed a linear increase relationship between the exhaust gas and the hydrogen flow rate. For instance, blending 20% hydrogen with 100% cottonseed oil methyl ester revealed and increase of (16.66 %) in exhaust gas temperature, (16.11%) BTE, (21.85 %) heat release rate, (40.51 %) Nitrogen monoxide emissions and (4.18 %) peak values for in-cylinder pressure compared to pure diesel. However, apparent drop in the effective compression ratio, volumetric efficiency, cut-off ratio, emissions of HC, CO and CO_2 were seen with the increase of hydrogen rates. Santos et al. [34] numerically investigated the effects of adding fractions of biodiesel of (12%, 15%, 18%, and 21%) and mix it with diesel. The finding of this study showed high fluctuations in isoalkanes and alkanes. However, no significant difference in interactions were seen for other molecules. Thus, the numerical model showed that the physical parameters blending biodiesel with diesel to a rate of (21%) insignificantly influence the viscosity and density. Peng et al. [35] produced soybean biodiesel using a new nano-catalyst (MGO@SnO) with various physical/chemical properties by combining (graphene oxide) shielded with magnetic-iron-oxide (MGO) and tin-oxide (SnO(x)) nanoparticles. It was found that the new catalyst was able to create the carbocation-ions to outbreak with methanol, then, producing methyl ester from triglycerides. In addition, reaction parameters were: molar-ratio of (soybean oil/ methanol) of (1:10), temperature of reaction (120 °C), ratio of (MGO/SnO) of (1:0.5) and period of reaction of (180 min). The performance of the new catalyst (MGO@SnO) showed good value of (> 88%).

The current study aims to investigate the effect of using biodiesel derived in soybean oil in constant speed, four stroke direct injection diesel engine numerically with the use of simulation software Diesel-RK

1. Materials and Methods

Table.1 illustrates the carbon and hydrogen contents, viscosity, density, cetane number, flash point and Calorific value of standard diesel fuel and SME blends. Table.2 shows the operating conditions and engine features used in the validation part.

Table.1: Characteristics of Diesel fuel, Soy-bean methyl ester and 20%-Soy-bean methyl ester.

Characteristic	Deisel (DF)	SME	20%SME
Chemical elements	$C_{13.77}$, $H_{23.44}$	C_{19}, H_{35}, O_2	$C_{14.97}$, $H_{26.33}$, $O_{0.34}$
Viscosity at 40 °C (cst)	3.0	4.25	3.34
Density at 15 °C (kg/m^3)	830	876	841
Cetane number	48	51.3	48.69
Flash point ($^{\circ}$C)	76	130	86.8
Calorific value (MJlkg)	42.5	36.22	41.18

Table.2: Specifications of (Kirloskar TAF-1) diesel engine used in this study.

Type of engine	Four strokes
Number of cylinders	Single
bore×stroke	87.5 mm×110 mm
Cylinder capacity	0.66L
Compression ratio	15, 16, 17.5 and 19
Rated power	4.4 kW at 1500 rpm
Max. torque (T_{max})	28 Nm at 1500 rpm
Orifice diameter (O.D)	150 μm
Time of injection (t_{inj})	20^0 BTDC
Pressure of injection (P_{inj})	220 bar

2. Numerical Analysis

A diesel-RK solver version 4.3.0.189 was hired to solve the governing equations and a model of multizone combustion was employed and formulated in this work [36, 37].

3.1 Conservation equations

As shown in equation (1), the total mass flow across an open system is conserved.

$$\frac{dm}{dt} = \sum_i m_i \quad (1)$$

where mi denotes the mass flow rate of each species

The analytical equation for species conservation is shown in Equation (2)

$$Y_i = \sum_i \frac{m_i}{m} \quad (2)$$

Where Yi represents the mass fraction of each species.

Open thermodynamic systems can be expressed by the subsequent standard energy formula:

$$\frac{d(mu)}{dt} = -p\frac{dv}{dt} + \frac{dQ_{ht}}{dt} + \sum_i m_i h_i \quad (3)$$

Equation (3) indicates the energy change rate on the left side, while the entropy flux, heat transfer rate, and displacement work rate are shown on the right side.

3.2 Model of Spray Assessment

The model is depending on the elementary fuel mass (EFM). The speed of transformation of EFM between injectors over a small-time interval and then directed to the spray tip. The EFM can be represented by Equation (4) and shown in Fig. 1.

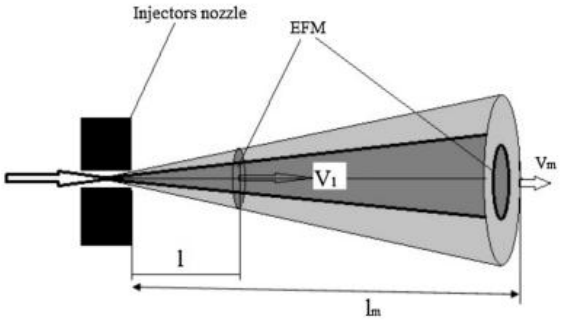

Figure 1. Fuel-spray representation [38].

$$\left[\frac{V}{V_0}\right]^{\frac{3}{2}} = 1 - \frac{l}{l_m}1 \quad (4)$$

Where: V– the EFM instantaneous speed, V◦– the EFM initial speed at the nozzle-injector, l– the space between the nozzle-injector and the EFM, l_m– the length of penetration of (EFM) measured to the end front a spray. The equation (4) is partially solved as:

$$3l_m\left[1-\left[1-\frac{l}{l_m}\right]^{0.333}\right]-V_o\tau_k=0 \quad (5)$$

Where:(τ_k) is the departure time for the (EFM) to amount to the length $(l\ )$from the nozzle-injector when the (EFM) is stopped at a spray-tip, then $l = l_m$ and $\tau_k = \tau_m$. Where (τ_m) is the departure time for the (EFM) to amount to the front of spray before ending. Equation (5) can be rewriter as:

$$l_m = V_o\ \frac{\tau_m}{3} \quad (6)$$

By employing equations (4) to (6) the present speed and the (EFM) length can be achieved as:

$$V = V_o\left[1-\frac{\tau_k}{\tau_m}\right]^2 \quad (7)$$

$$l = l_m\left[1-\left[1-\frac{\tau_k}{\tau_m}\right]^3\right] \quad (8)$$

Several dimensionless parameters are introduced to calculate the geometry of the spray which account for the design parameters of the injector and physical properties of the fuel, namely Weber number; square ohenzorge number. In modeling the fuel spray behavior, it is assumed that its evolution occurs in two phases, namely initial (a) and main (b). The boundary between these two phases is denoted by lg, and the period of time for the jet to reach this boundary by tg. Further details can be found in Mahkamov K. et al. [39].

3.3 Model of Heat Release

For computing the heat release at a single cycle, there are two assumptions [40]:

1. The diesel fuel evaporation speed in each zone and the total speed of the separate diesel fuel droplets evaporation are equal.
2. During the injection of the diesel fuel, the ratio of evaporation constant to initial droplet diameter is fixed.
3. The combustion process can be split into four stages, in which each stage has particular chemical and physical characteristics restricting the burning rate-speed.

Stages are described below [41]:

The period of the ignition delay stage is obtained by:

$$\tau = \sqrt{\frac{T}{P}} * e^{\left(\frac{E_a}{8{,}312T} - \frac{70}{CN+25}\right)} * 3.8 * 10^{-6} * (n * 1 - 1.6 * 10^{-4}) \quad (9)$$

Stage of Premixed-combustion, where the combustion-process of the blend of air and the fuel-vapor occurred by the combustion:

$$\frac{dx}{dt} = \varphi_1 \left(\frac{d\sigma_u}{d\tau}\right) + \varphi_o * \left[(\sigma_{ud} - x_o)(0.1\sigma_{ud} + x_o)A_o \left(\frac{m_f}{V_i}\right)\right] \quad (10)$$

Stage of diffusive-combustion where the blended fuel is injected and directly combusted

$$\frac{dx}{d\tau} = \varphi_2 \left((\sigma_u - x)(\emptyset - x) * A_2 \left(\frac{m_f}{V_c}\right)\right) + \varphi_1 \left(\frac{d\sigma_u}{d\tau}\right) \quad (11)$$

Late burning stage (the fuel burning after the completed injection):

$$\frac{dx}{d\tau} = (1 - x)(\varepsilon_b \emptyset - x) * \varphi_3 K_T A_3 \quad (12)$$

$\varphi_3 = \varphi_2 = \varphi_1 = \varphi_o$ Representing a function that expresses the completion of the combustion of fuel vapor in zones:

$$\phi = 1 - (A_1/\varepsilon_b \emptyset - x)\frac{dx}{dt} \left\{ r_v + \sum_{i=1}^{m_w} \left[r_{wi} * 300 * e^{\left(\frac{-16000}{2500 + r_{wi}}\right)} \right] \right\} \quad (13)$$

Where:(ε_b) represents the efficiency of using air, (r_v) describes the proportion of relative-evaporation in the environment-zones and front, (ϕ) describes the proportion of equivalence, (r_{wi}) describes the proportion of the related-evaporation during different zones inside wall-surface flow.

3.4 Model of NOx formation

Normally, the emissions of NOx consist of a mixture of both NO and NO_2. The current work hired the mechanism of (Zel'Dovich) within the solver of the Diesel-RK program to evaluate the emissions of Nox [42]:

$$O_2 \leftrightarrow 2O \quad (14)$$

$$O + N_2 \leftrightarrow NO + N \quad (15)$$

$$O_2 + N \leftrightarrow NO + O \quad (16)$$

The concentration of atomic-oxygen influences the reaction-rate as shown in Equation. 16. The concentration volume of NO is calculated using the equation:

$$\frac{d[NO]}{d\theta} = \frac{e^{-38020/T_z}[N_2]_e[O]_e\left(1-\left(\frac{[NO]}{[NO]_e}\right)^2\right)*2.33*10^7 P}{RT_z\left[1+\left(2365/T_z\right)e^{3365/T_z}[NO]/[O_2]_e\right]}\left[\frac{1}{rps}\right] \quad (17)$$

3.5 Modelling of Soot concentration

The definition of soot is a tiny black (carbon particle) in the vapor carrier existence, that is produced due to the incomplete combustion-process of hydrocarbon. Modeling of soot can be found in detail in the literature [43].

The concentration of soot in the exhaust relative to the normal operating conditions is described as:

$$[C] = \int_{\theta_B}^{480} \frac{d[C]}{d\tau}\frac{d\theta}{6n}\left[\frac{0.1}{P}\right]^{\gamma} \quad (18)$$

Hartidge smoke level was determined using the equation (19):

$$\text{Hartidge} = 100 * \left[1 - e^{(-24226[C])} * 0.9545\right] \quad (19)$$

Equation (20) was employed to calculate the Particulate Matter [PM] as a function of [BSN]:

$$[PM] = 565 * \left[\ln\frac{10}{10-Bosch}\right]^{1.206} \quad (20)$$

The combination of pollutants [PM] and [NOx] that describes the air pollutant emission [SE] [44]:

$$SE = C_{PM}\left[\frac{PM}{0.15}\right] + C_{NO}\left[\frac{NO_x}{7}\right] \quad (21)$$

4. Software Validation

By comparing the Diesel-RK software's output with the findings of A.J. Reiter's study [45], its correctness is verified. Identical engine specifications and operational circumstances are employed, as Table 3 illustrates. Fig. 2 displays the pressure growth curve across each crank angle. On an energy base, the turbocharged engine is operated in dual fuel setting, using 60% diesel and 40% ammonia. Comparing the current analysis to that of A.J. Reiter [30], the trends are found similar with just a 5% variance. The current work revealed a pressure of 7.46 MPa at 5 deg. ATDC, whereas the highest pressure of 7.83 MPa appears at 6º ATDC. The influence of replacing NH_3 in diesel on the volumetric concentration of CO_2 is seen in Fig. 3. With only a small variance, each curve appears to have a matching posture. For diesel with a single fuel (100% operation). The values obtained for (60% diesel+40% NH_3) on dual fuel mode differ by 6%, while the CO_2 concentration deviates by 2.083% from those reported by A.J. Reiter [45]. It's important to note that the simulation program is reliable enough and works well as a tool to model the combustion process in diesel engines.

Table 3: Engine data utilized for verification [45].

Technical details	Information
Engine brand	4045TT068
Engine type	In-line, 4-stroke
Bore and stroke	106 x 127 (mm)

Compression ratio	17:1
Aspiration	Turbocharged
Injection system	Standyne DB4 rotary pump
Engine speed	1000 rpm
Peak power	66 kW @2100 rpm
Peak torque	387 N.m @1300 rpm
Fuel	nH4oh+Diesel

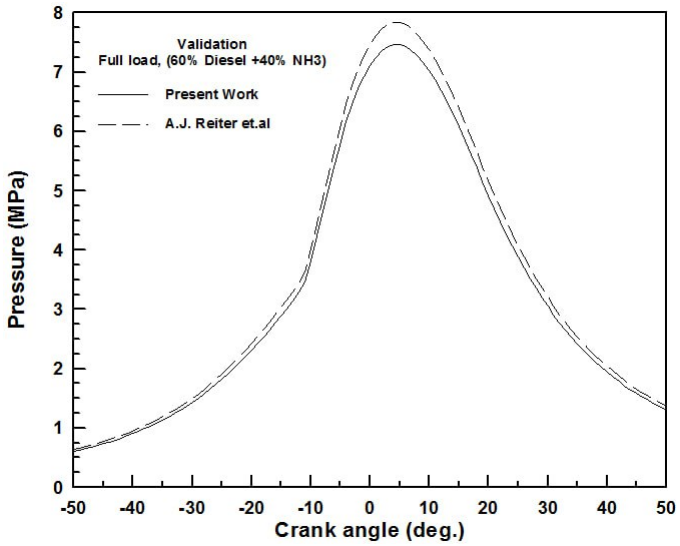

Figure 2. Validation of cylinder pressure profile

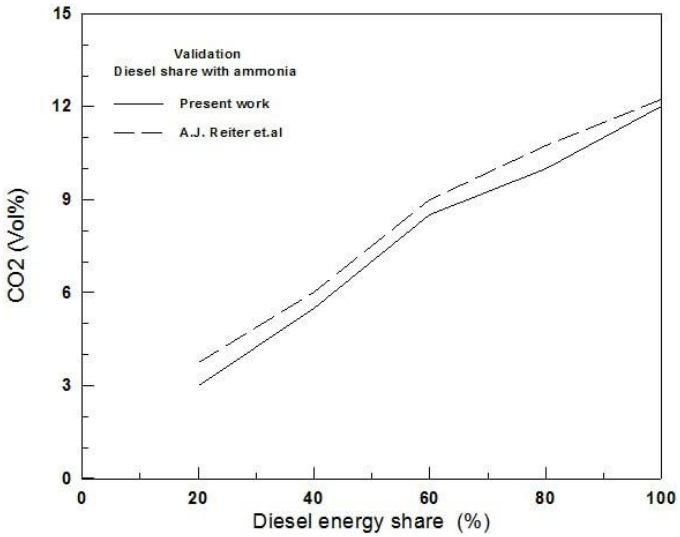

Figure 3. Validation of CO_2 concentration per % diesel energy.

5. Results and Discussion

5.1 Combustion Study

Fig. (4) presents the change of cylinder pressure with crank's angle at full load for fuel, 20%SME and neat SME. Since all curves investigated have the same distribution closer to each other, only the duration of 150^o crank angles is selected starts from 300^o to 450^o as shows dramatic changes among each other is seen easily. Obviously, the cylinder pressure for the biodiesel fuel is less than

the one of the used diesel fuel because of the difference in the heating value for the blended fuel. In addition, the peak pressure gained for pure SME is 71.25 bar at 6o crank angle is closer to top dead center (TDC) relative to classic diesel fuel where the maximum pressure was 100.71 bar at 4o crank angle BTDC. Also, it can be observed that 20% SME pressure is very close to the pressure of pure diesel.

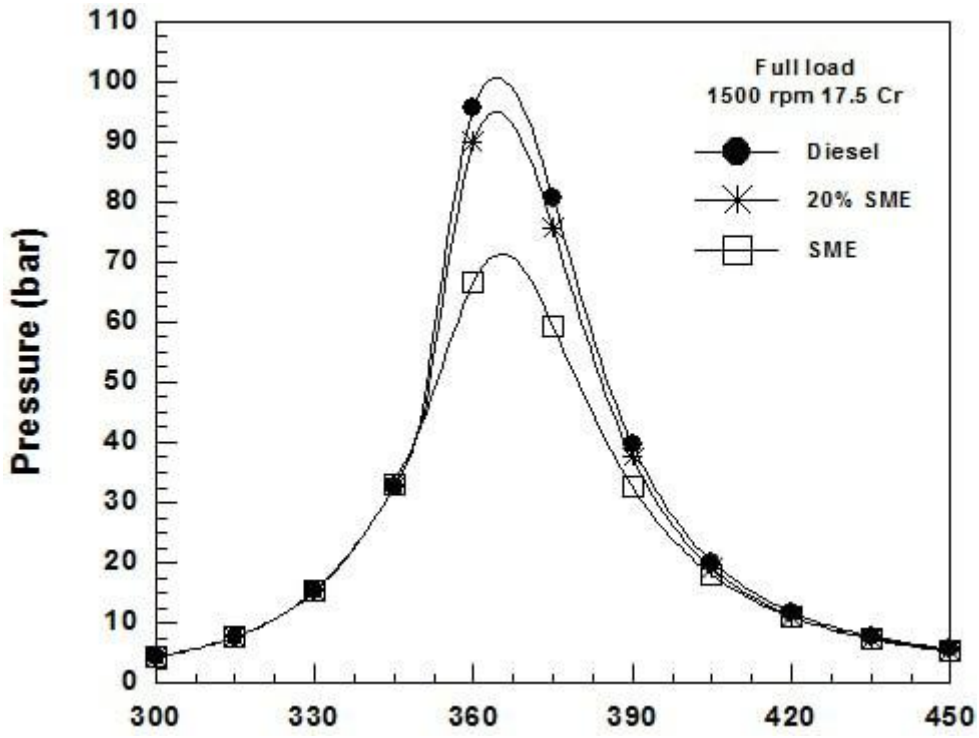

Figure (4) The cylinder pressure vs crank angle for diesel, 20%SME and SME at full load.

Figure (5) shows the integral heat release rate with crank angle at full load. Obviously, the amount of heat release rate decreases when SME blends increased due the reduction in energy content of SME compared to base line diesel. SME biodiesel had quicker start of combustion, while combustion rate is slower. This is because of the acceleration in the injection timing and shorter ignition delay. Where it influences the fuel compression process in the volumetric injection pump. Therefore, the needle nozzle is raised faster when utilizing the biodiesel fuel that makes acceleration in the beginning of injection timing[46]. In addition, the higher bulk modulus of methyl esters of vegetable oils leads to accelerate the injection process [47]. Moreover, the auto-ignition of any fuel with a high cetane number will be easy, and the ignition delay of that fuel will be short. That means the cetane number of diesel fuel is lower than the one of biodiesel. On the other hand, the relation between the aromatic compounds of the fuel and the ignition delay is proportional[48]. Therefore, the ignition delay of biodiesel is shorter because the amount of aromatic compounds in the biodiesel is lower than that in the diesel.

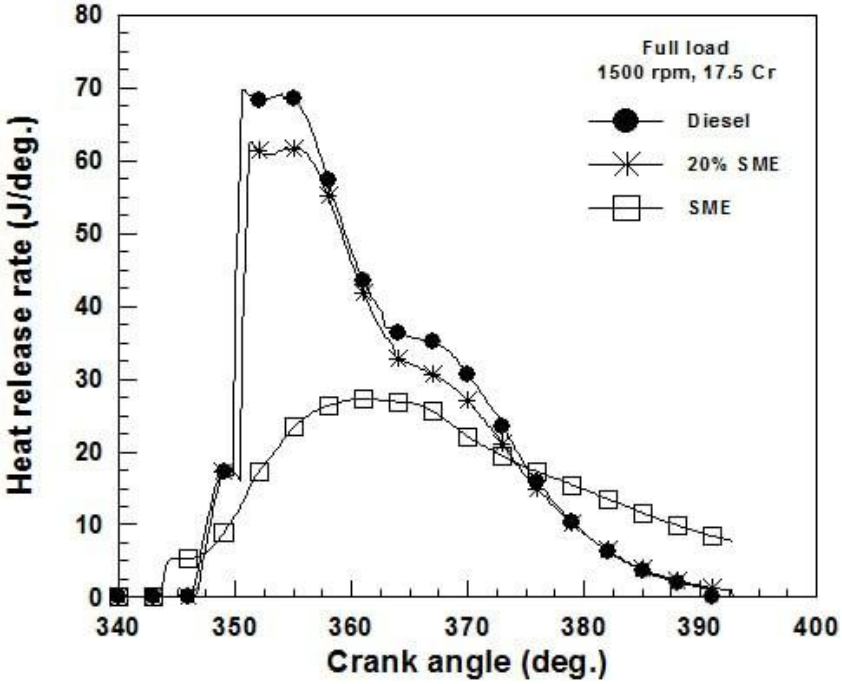

Figure (5) The heat release vs crank angle for diesel, 20%SME and SME at full load.

It can be concluded that this is a promising technology for achieving better thermal efficiency and controlling both NOX and smoke emissions. This technology can be introduced in the existing conventional compression ignition engines with no engine hardware modifications, thus leading to saving of precious diesel fuel and saving the human and plant life from the hazardous effects of exhaust gas pollutants from the diesel engines can be achieved. It is also hoped that the new data presented here will help in developing new predictive methods or procedures for this problem.

Fig. (6) illustrates the values of SMD for diesel, 20%SME and pure SMD. Owing to the increase in the SME fraction in the used fuel, the SMD increases. The specific reason behind that is the increase in the SME fraction in the used fuel leads to increase the surface tension and viscosity coefficients. That means the droplets diameter of biodiesel will be increased which leads to decrease the burning rate and evaporation speed of the used fuel. Compared to diesel the SMD is increased by 8.7% and 24% for the use of 20% SME and SME respectively.

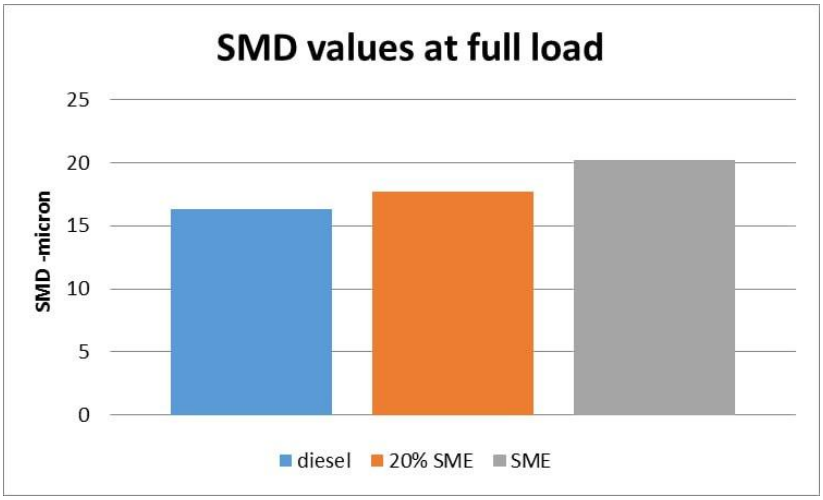

Figure (6) The SMD values for diesel, 20%SME and SME at full load.

The variation of the ignition delay values is displayed in Fig.(7). The ID-degree of pure SME is the smallest because the cetane number of the pure SME is the higher. While the ID-degree of used diesel fuel is higher than that for the ID-degree of pure SME. This is because the cetane number of the used diesel is lowest. But the combination of diesel fuel and biodiesel fuel (20%SME) gives the highest ID-degree. The same results were reported by [49]. While the ignition delay of standard diesel is 10^{o} crank angle, it was 9.35^{o} and 3.2^{o} for 20%SME and pure SME consequently.

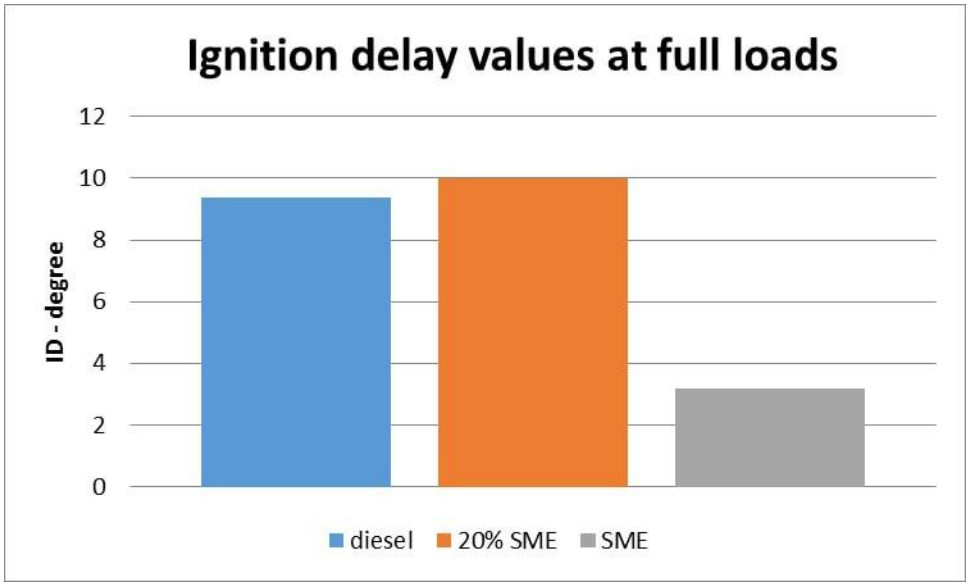

Figure (7) The ignition delay for diesel, 20%SME and SME at full load.

The next figure is the values of SOC which is influenced by ignition delay for the tested fuels. Since the use of SME instead of diesel leads to shorted ID, it is logically to observe an earlier SOC for all SME blends. The injection timing starts at 20^{o} BTDC, and according to the values of ID obtained in Fig. (8), hence, the SOC is 10^{o}, 10.35^{o} and 16.8^{o} BTDC respectively.

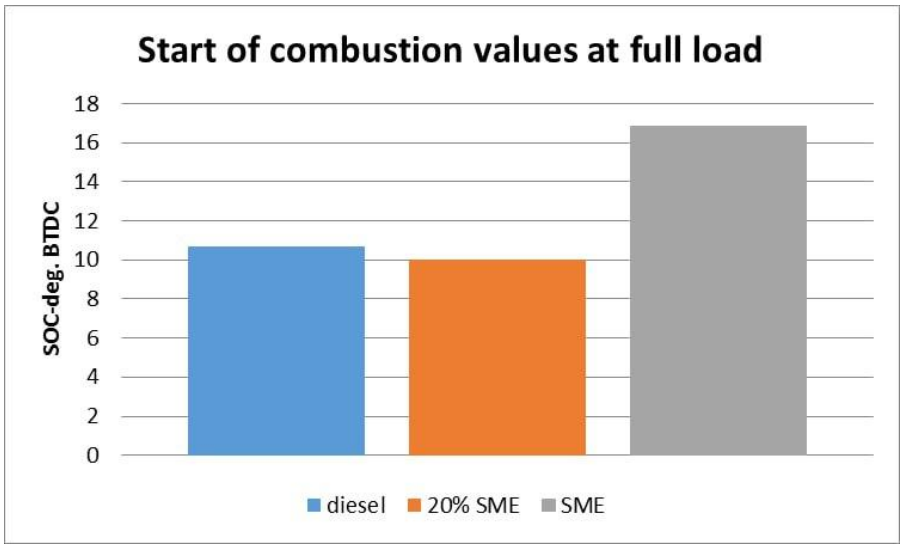

Figure (8) The SOC for diesel, 20%SME and SME at full load.

Fig. (9) presents the spray tip penetration with a crank angle. Tested fuels used for the investigations are diesel, 20% SME, and SME. A rapid increase in spray penetration is noticed through the initial stages of injection because of less reaction between droplets and nitrogen. The SME blends have higher spray penetration with respect to diesel. The difference in the density and viscosity levels is responsible for the trend; hence, the spray jet is prevented from breaking, resulting in an increase in the size of the spray droplets[50]. Hence, the spray penetration is lengthened, recording higher penetration for SME 86 mm while it was 83 mm for diesel.

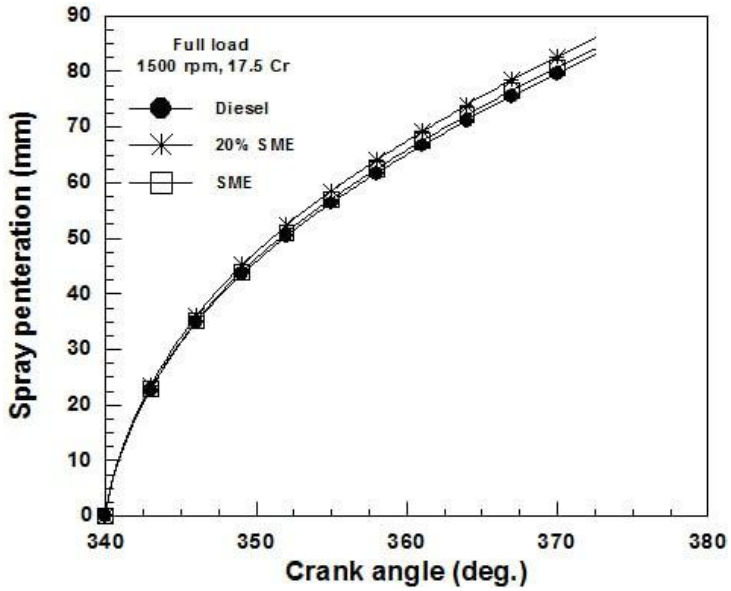

Figure (9) Spray penetration values vs crank angle for diesel, 20%SME and SME at full load.

Typical regions that undergo significant alterations during the combustion stage were studied. There are stoichiometric regions as well as lean and rich regions. The temperature profile of the zone is shown in Fig. (10), which is displayed. Because SME and diesel have different lower heating values than diesel, the zone temperature drops from 2877 K to 2672 K. This reduction can be considered as good sign for reduction in NOx emissions. Same observations are reported by [51].

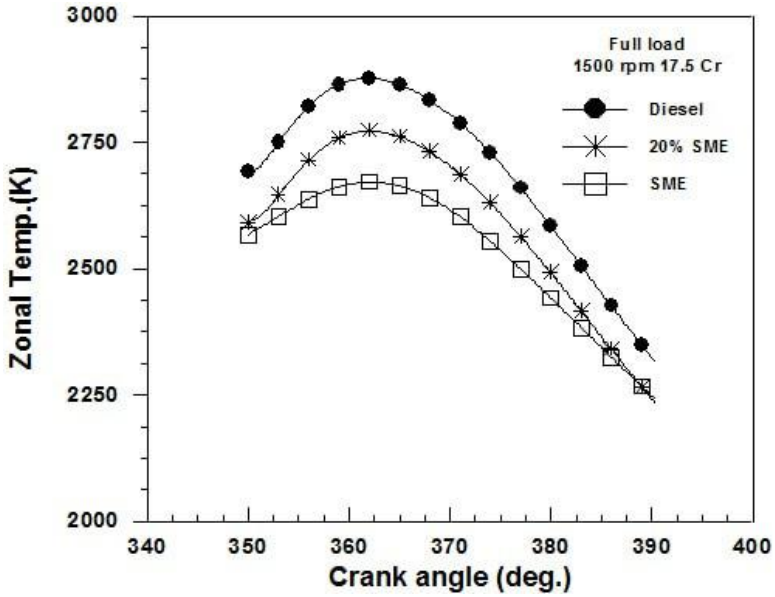

Figure (10) Zonal temp values vs crank angle for diesel, 20%SME and SME at full load.

Generally, NOx concentration increases suddenly with time and reaches its highest estimate before dropping somewhat because of the increase in oxygen concentration. This allows the temperature of the burned gas to mix with the air. The temperature drops later causing the concentration to freeze because the reaction cannot continue[51, 52].

The concentration of NO_X is depending on a variety of variables, such as the cylinder temperature, the proportion of oxygen present, and the amount of time necessary for the reaction to occur during combustion. The results obtained, see fig.(11), indicated a reduction in combustion temperature which leads to significant reduction NOx emissions. While the NOx of diesel is, 3744 ppm, it was 2670 pm, and 1250 ppm for 20% SME, and SME respectively.

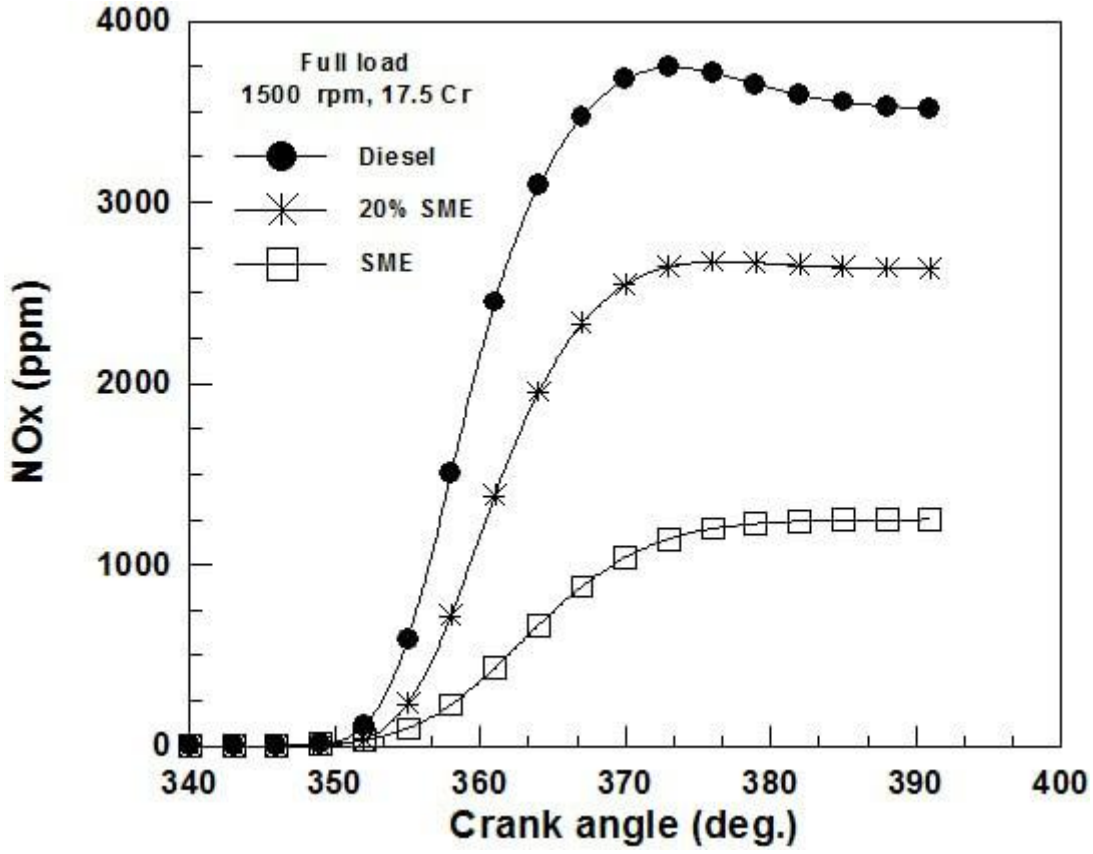

Figure (11) NOx values vs crank angle for diesel, 20%SME and SME at full load.

2.1.Performance study

Figs. (12) and (13) presents the difference of BTE and BSFC with diesel and biodiesel. It is observed that BTE of soy-bean blends were lower than that of pure diesel for the entire load by 0.8% and 6.2% for the use of 20% SME and pure SME, respectively. The decreasing trend in efficiency with increase in concentration of SME in diesel may be due to lower heating value of biodiesel over the nominal diesel fuel. It also may be caused by its poor atomization due to its high viscosity. The BSFC was found to increase with increasing the percentage of SME in the fuel.

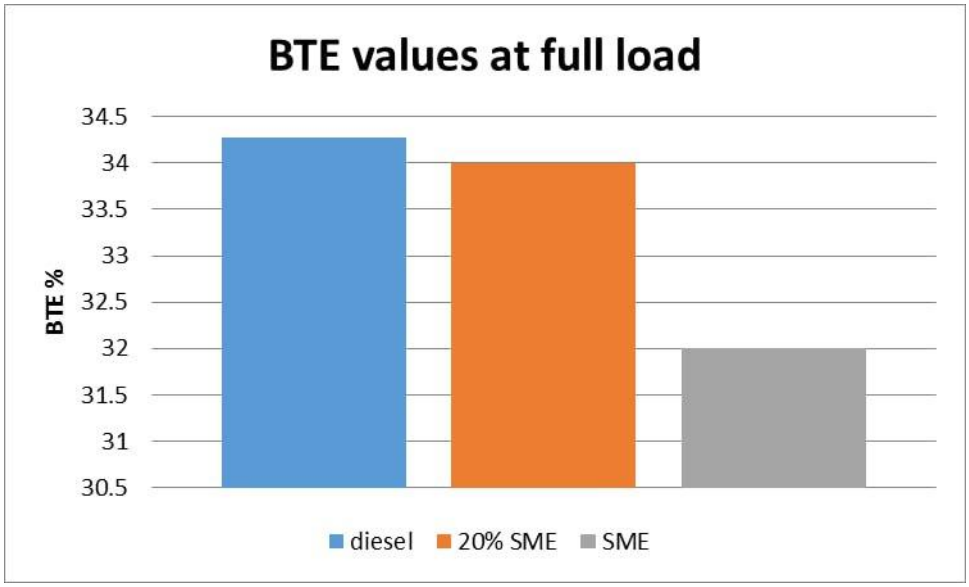

Figure (12) BTE values for diesel, 20%SME and SME at full load.

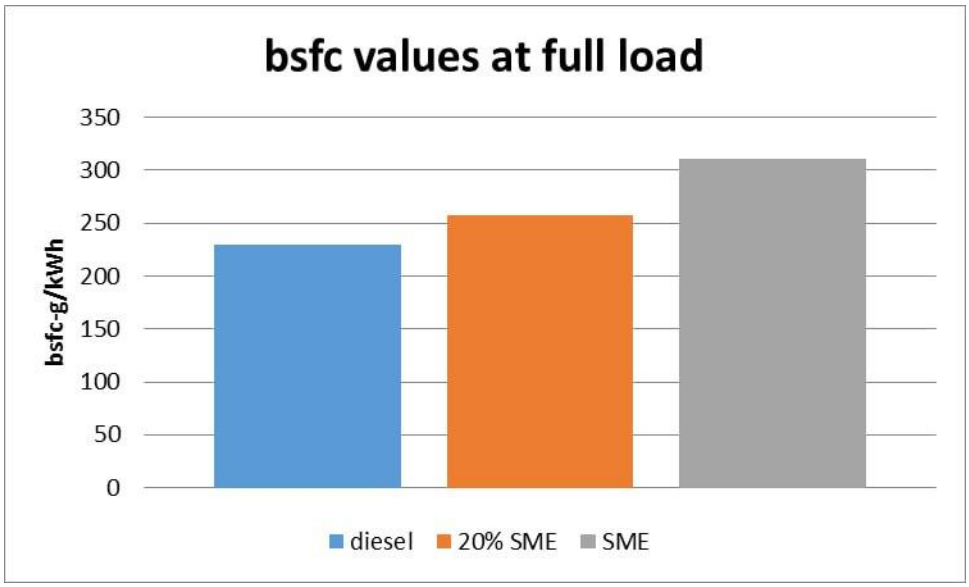

Figure (13) BSFC values for diesel, 20%SME and SME at full load.

To obtain the same torque and power output for each fuel tested, the BSFC was higher for SME and its blends. BSFC for B20 SME is higher than diesel fuel by 11.95%, while it is higher by 35.38% for neat SME. The increase in BSFC is due to higher density and lower heating value, since methyl esters have heating values that are about 12.4% less than pure diesel. These results are similar to those of [53] [54].

2.2.Emission study

Emissions of CO_2 and NOx are also important for measuring the quality of air and their influence on the environment. The quantity of CO_2 produced by burning SME, 20% SME and diesel is illustrated in Fig. 14. The SME emits extra CO_2 compared to 20% SME and the diesel recorded the lowest value. The high CO2 emissions can be attributed to the higher density. The values of

CO_2 emissions for SME, 20% SME and diesel fuel blends are (759.62 kg/kWh), (818.58 kg/kWh) and (870.461 kg/kWh) respectively.

Fig. 14 demonstrates a comparison of the NOx levels for SME, 20% SME and diesel fuel blends. The Nox represent an important factor periodic examination of the vehicles[55]. The obtained results showed that pure SME and 20 % SME produced lower NOx level compared to diesel fuel of nearly (15.53 kg/kWh) and (26.3 kg/kWh) respectively. Nevertheless, diesel fuel produced the highest NOx level of (31.34 kg/kWh).

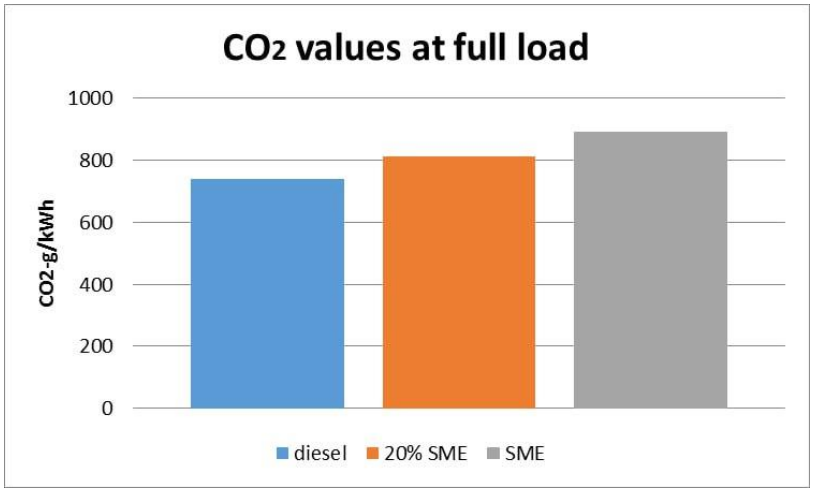

Figure 14. CO2 values at full load

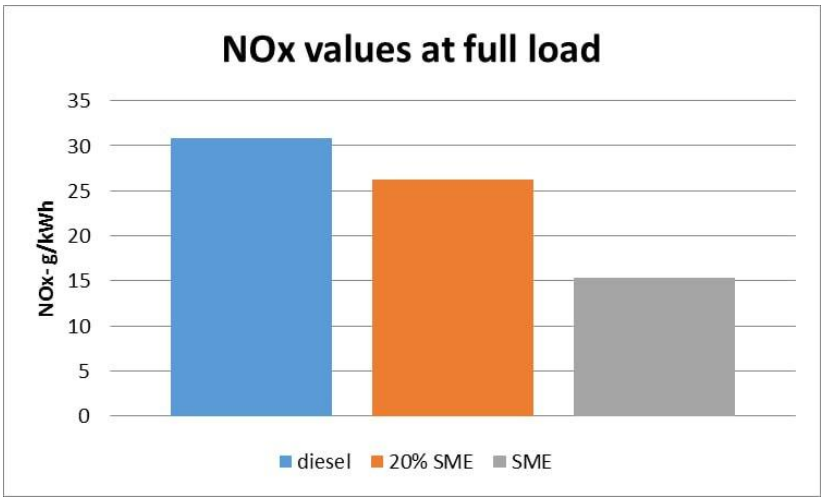

Figure 15. NOx values at full load.

3. Conclusions

1. The use of SME blends tends to have a higher cetane number, which can improve combustion efficiency and reduce ignition delay.
2. The oxygen content in SME promotes more complete combustion,
3. The BSFC increased slightly with the SME blends, indicating a slight decrease in fuel efficiency compared to diesel and pure SME.
4. Engine efficiency decreased, but this is often within acceptable limits and can be offset by

the environmental benefits.

5. Compared to pure diesel, the use of 20% SME and pure SME reduced NOx emissions significantly by 15% and 50 % respectively.
6. Even the use of SME blends may slightly reduce fuel efficiency and increase CO_2 emissions, but they offer significant benefits in terms of reduced NO_x emissions, contributing to improved air quality and environmental sustainability.
7. The current study recommends the use of 20% SME as an alternative source of energy in diesel engine
8. This investigation should be followed by optimization study of using SME blends in diesel engine subjected to different loading and operating conditions.

References

1. Al-Obaidi, W., M.F. Al-Dawody, and K. Al-Farhany, Effect of Hybrid Fuels of Aqueous Ammonia, Dimethyl Ether, Biodiesel and Diesel Fuel on Thermal Performance of Diesel Engine. International Journal of Heat and Technology, 2024. **42**(3): p. 812-822.
2. Delfanian, M., et al., Interfacial behavior of gallic acid and its alkyl esters in stripped soybean oil in combination with monoacylglycerol and phospholipid. Food Chem, 2023. **413**: p. 135618.
3. Al-Obaidi, W.J.K. and W. Jamshed, A numerical study of the effects of various diesel fuel types on the performance of single-cylinder diesel engines. Al-Qadisiyah Journal for Engineering Sciences, 2024. **17**(4): p. 436-444.
4. Shrivastava, P. and T.N. Verma, Effect of fuel injection pressure on the characteristics of CI engine fuelled with biodiesel from Roselle oil. Fuel, 2020. **265**: p. 117005.
5. Gupta, P., et al., Impact of fuel injection pressure on the common rail direct fuel injection engine powered by microalgae, kapok oil, and soybean biodiesel blend. Industrial Crops and Products, 2023. **194**: p. 116332.
6. Bortel, I., J. Vávra, and M. Takáts, Effect of HVO fuel mixtures on emissions and performance of a passenger car size diesel engine. Renewable Energy, 2019. **140**: p. 680-691.
7. Teoh, Y.H., et al., Comparative assessment of performance, emissions and combustion characteristics of tire pyrolysis oil-diesel and biodiesel-diesel blends in a common-rail direct injection engine. Fuel, 2022. **313**: p. 123058.
8. Arunkumar, M., et al. A Study on Performance and Emission Characteristics of Diesel Engine Using Ricinus Communis (Castor Oil) Ethyl Esters. Energies, 2021. **14**, DOI: 10.3390/en14144320.
9. Dharmalingam, B., et al., A review on different additives and advanced injection strategy on diesel engine characteristics fuelled with first, second and third generation biodiesel. Materials Today: Proceedings, 2023. **72**: p. 2909-2914.
10. Wyatt, V.T. and M.J. Haas, Production of Fatty Acid Methyl Esters via the In Situ Transesterification of Soybean Oil in Carbon Dioxide-Expanded Methanol. Journal of the American Oil Chemists' Society, 2009. **86**(10): p. 1009-1016.
11. Vázquez-Garrido, I., A. Guevara-Lara, and A. López-Benítez, Hydroprocessing of new and waste soybean oil for obtaining biodiesel: An operational conditions study. Chemical Engineering Journal, 2023. **452**: p. 139508.

12. He, P., et al., Two-dimensional Mo catalysts supported on the external surface of planar Silicalite-1 zeolite for biodiesel production from waste cooking soybean oil: Transesterification experiment and kinetics. Fuel, 2024. **360**: p. 130610.
13. De Poures, M.V., et al., Collective influence and optimization of 1-hexanol, fuel injection timing, and EGR to control toxic emissions from a light-duty agricultural diesel engine fueled with diesel/waste cooking oil methyl ester blends. Process Safety and Environmental Protection, 2023. **172**: p. 738-752.
14. Elkelawy, M., et al., Maximization of biodiesel production from sunflower and soybean oils and prediction of diesel engine performance and emission characteristics through response surface methodology. Fuel, 2020. **266**: p. 117072.
15. Mora, J.M.R., et al., Biodiesel production from soybean oil via LiOH-pumice catalytic transesterification and BBD-RSM optimization. Energy Reports, 2024. **11**: p. 4032-4043.
16. Santos Sonnemberg, M.N., et al., Investigation of curcumin antioxidant efficiency on oxidation stability of biodiesel from soybean oil and beef tallow, contaminated with metals: Kinetic and storage studies. Fuel, 2024. **368**: p. 131520.
17. Aleman-Ramirez, J.L., et al., Agro-industrial residue of Pouteria sapota peels as a green heterogeneous catalyst to produce biodiesel from soybean and sunflower oils. Renewable Energy, 2024. **224**: p. 120163.
18. Ağbulut, Ü., et al., Production of waste soybean oil biodiesel with various catalysts, and the catalyst role on the CI engine behaviors. Energy, 2024. **290**: p. 130157.
19. Zhong, W., et al., Experimental study on combustion and emission characteristics of fatty acid methyl esters and hydrogenated catalytic biodiesel/diesel blends under world harmonized steady state cycle. Fuel, 2023. **343**: p. 127887.
20. Gavhane, R.S., et al. Influence of Silica Nano-Additives on Performance and Emission Characteristics of Soybean Biodiesel Fuelled Diesel Engine. Energies, 2021. **14**, DOI: 10.3390/en14051489.
21. Kumar Deb, B. and P. Chakraborti, Multi-response optimization of the performance and emission characteristics of a diesel engine fueled with palm kernel oil methyl ester using TOPSIS-RSM hybrid approach. Materials Today: Proceedings, 2023.
22. Zhang, L., et al., Development of a reduced oxidation mechanism with low-temperature chemistry for real biodiesel methyl esters. Fuel, 2023. **338**: p. 127289.
23. Hasnain, S.M.M., et al., Investigation and impact assessment of soybean biodiesel, methyl oleate, and diesel blends on CRDI performance and emissions. Materials Science for Energy Technologies, 2024. **7**: p. 124-132.
24. Ramalingam, S., et al., Environmental and energy valuation of waste-derived Cymbopogon Martinii Methyl Ester combined with multi-walled carbon (MWCNTs) additives in hydrogen-enriched dual fuel engine. International Journal of Hydrogen Energy, 2023. **48**(99): p. 39641-39657.
25. Al-Dawody, M.F., et al., Effects of mixing tallow methyl ester with diesel fuel on the thermal characteristics of diesel engine. Energy Conversion and Management: X, 2024. **24**: p. 100804.
26. Yusuff, A.S., et al., Experimental investigation of influence of methyl, ethyl and methyl-ethyl ester blends of used cooking oil on engine performances and emissions. Energy Conversion and Management: X, 2023. **17**: p. 100346.

27. Al-Iessa, A.A.H., A. Abdollahi, and H. Soleimanimehr, Investigating the atomic and thermal performance of soy biodiesel methyl ester in the presence of hybrid CuO/Al2O3 nanoparticles by molecular dynamics simulation. Engineering Analysis with Boundary Elements, 2023. **151**: p. 8-18.
28. Passos, R.M.d., et al., Ethyl biodiesel production from crude soybean oil using enzymatic degumming-transesterification associated process. Industrial Crops and Products, 2024. **222**: p. 119930.
29. dos Passos, R.M., et al., Phospholipase cocktail: A new degumming technique for crude soybean oil. LWT, 2022. **159**: p. 113197.
30. Kumar, S. and S. Bansal, Performance evaluation of ANFIS and RSM in modeling biodiesel synthesis from soybean oil. Biosensors and Bioelectronics: X, 2023. **15**: p. 100408.
31. Chen, Y., et al., The combustion process of methyl ester-biodiesel in the presence of different nanoparticles: A molecular dynamics approach. Journal of Molecular Liquids, 2023. **373**: p. 121232.
32. Tosun, E. and M. Özcanlı, Hydrogen enrichment effects on performance and emission characteristics of a diesel engine operated with diesel-soybean biodiesel blends with nanoparticle addition. Engineering Science and Technology, an International Journal, 2021. **24**(3): p. 648-654.
33. Gurusamy, M. and B. Subramanian, A comprehensive analysis of a dual fuel engine operating on cottonseed oil methyl ester and hydrogen. Fuel, 2025. **383**: p. 133789.
34. Santos, A.L.R., et al., Study of molecular arrangement and density estimation of soybean oil biodiesel-diesel blends employing molecular dynamic simulation. Fuel, 2024. **377**: p. 132760.
35. Peng, L., et al., Magnetic graphene oxide supported tin oxide (SnO) nanocomposite as a heterogeneous catalyst for biodiesel production from soybean oil. Renewable Energy, 2024. **224**: p. 120050.
36. Al-Dawody, M.F. and S.K. Bhatti, Optimization strategies to reduce the biodiesel NOx effect in diesel engine with experimental verification. Energy Conversion and Management, 2013. **68**: p. 96-104.
37. Al-Dawody, M.F. and M.S. Edam, Experimental and numerical investigation of adding castor methyl ester and alumina nanoparticles on performance and emissions of a diesel engine. Fuel, 2022. **307**: p. 121784.
38. Al-Dawody, M.F. and S. Bhatti, Optimization strategies to reduce the biodiesel NOx effect in diesel engine with experimental verification. Energy conversion and management, 2013. **68**: p. 96-104.
39. Kuleshov, A. and K. Mahkamov, Multi-zone diesel fuel spray combustion model for the simulation of a diesel engine running on biofuel. 2008. **222**(3): p. 309-321.
40. Hiroyasu, H., T. Kadota, and M. Arai, Supplementary Comments: Fuel Spray Characterization in Diesel Engines. Combustion Modeling in Reciprocating Engines, 1980: p. 369-408.
41. Al-Amir, Q.R., M.F. Al-Dawody, and A.m. Abd, Design of Cooling System for an Automotive using Exhaust Gasses of Turbocharged Diesel Engine. Journal of The Institution of Engineers (India): Series C, 2022. **103**(3): p. 325-337.
42. Al-Dawody, M.F., et al., Mechanical engineering advantages of a dual fuel diesel engine powered by diesel and aqueous ammonia blends. Fuel, 2023. **346**: p. 128398.

43. Kuleshov, A., Model for predicting air-fuel mixing, combustion and emissions in DI diesel engines over whole operating range. 2005, SAE Technical Paper.
44. Kuleshov, A., Use of multi-zone DI diesel spray combustion model for simulation and optimization of performance and emissions of engines with multiple injection. 2006, SAE Technical Paper.
45. Reiter, A.J. and S.-C. Kong, Combustion and emissions characteristics of compression-ignition engine using dual ammonia-diesel fuel. Fuel, 2011. **90**(1): p. 87-97.
46. Ozsezen, A.N. and M. Canakci, Determination of performance and combustion characteristics of a diesel engine fueled with canola and waste palm oil methyl esters. Energy Conversion and Management, 2011. **52**(1): p. 108-116.
47. Boehman, A.L., et al., The Impact of the Bulk Modulus of Diesel Fuels on Fuel Injection Timing. Energy & Fuels, 2004. **18**(6): p. 1877-1882.
48. Stringer, F.W., A.E. Clarke, and J.S. Clarke, The Spontaneous Ignition of Hydrocarbon Fuels in a Flowing System. 1969. **184**(10): p. 212-225.
49. Yuan, W. and A. Hansen, Computational investigation of the effect of biodiesel fuel properties on diesel engine NOx emissions. International Journal of Agricultural and Biological Engineering, 2009. **2**: p. 41-48.
50. Al-Dawody, M., et al., Numerical study for the spray characteristics of diesel engine powered by biodiesel fuels under different injection pressures. Journal of Engineering Research, 2022. **10**(1B): p. 264-289.
51. Al-Dawody, M.F., et al., Using oxy-hydrogen gas to enhance efficacy and reduce emissions of diesel engine. Ain Shams Engineering Journal, 2023. **14**(12): p. 102217.
52. F. Al-Dawody, M. and s.K. Bhatti, Effect of variable compression ratio on the combustion, performance and emission parameters of a diesel engine fuelled with diesel and soybean biodiesel blending. World Applied Sciences Journal, 2014. **30**: p. 1852-1858.
53. Monyem, A. and J. H. Van Gerpen, The effect of biodiesel oxidation on engine performance and emissions. Biomass and Bioenergy, 2001. **20**(4): p. 317-325.
54. Canakci, M. and J. Gerpen, Comparison of Engine Performance and Emissions for Petroleum Diesel Fuel, Yellow Grease Biodiesel, and Soybean Oil Biodiesel. Transactions of the ASAE, 2003. **46**.
55. Franzetti, J., et al., Measuring NOx during periodic technical inspection of diesel vehicles. Environmental Sciences Europe, 2024. **36**(1).